Article

Journal of Vibration and Control
2019, Vol. 25(9) 1521–1535

DOI: 10.1177/1077546319827393
journals.sagepub.com/home/jvc
SAGE

An adaptive fuzzy sliding mode controller for uncertain underactuated mechanical systems

Wallace M. Bessa[1], Svenja Otto[2], Edwin Kreuzer[2] and Robert Seifried[2]

Abstract

Underactuated mechanical systems are frequently encountered in several industrial and real-world applications such as robotic manipulators with elastic components, aerospace vehicles, marine vessels, and overhead container cranes. The design of accurate controllers for this kind of mechanical system can become very challenging, especially if a high level of uncertainty is involved. In this paper, an adaptive fuzzy inference system is combined with a sliding mode controller in order to enhance the control performance of uncertain underactuated mechanical systems. The proposed scheme can deal with a large class of multiple-input–multiple-output underactuated systems subject to parameter uncertainties, unmodeled dynamics, and external disturbances. The convergence properties of the resulting intelligent controller are proved by means of a Lyapunov-like stability analysis. Experimental results obtained with an overhead container crane demonstrate not only the feasibility of the proposed scheme, but also its improved efficacy for both stabilization and trajectory tracking problems.

Keywords

Fuzzy logic, intelligent control, overhead crane, sliding modes, underactuated mechanical system

1. Introduction

A mechanical system is defined as underactuated if it has more degrees of freedom (DOFs) to be controlled than independent control inputs/actuators. Basically, underactuation can arise due to several reasons (Seifried, 2013): (i) intentionally, in view of design issues; (ii) owing to DOFs resulting from body elasticity; and (iii) upon actuator failure. Therefore, underactuated mechanical systems (UMS) can be commonly found in many branches of industrial activity.

Despite the broad spectrum of applications, ranging from robotic manipulators and overhead cranes to aerospace vehicles and watercrafts, the problem of designing accurate controllers for underactuated systems is, however, much more difficult than for fully actuated ones. For the class of underactuated multibody systems with nonintegrable constraints, controllability and stabilizability conditions are analyzed in Reyhanoglu et al. (1999).

In fact, the dynamic behavior of an UMS is frequently uncertain and highly nonlinear, which makes the design of control schemes for such systems a challenge for conventional and well-established methods. Pervozvanski and Freidovich (1999), for example, show that proportional–integral–derivative (PID) controllers are not the most suitable choice for underactuated systems. In these cases, only the actuated states can be easily stabilized by this type of controller. For the stabilization of all coordinates, however, the choice of the parameters is not straightforward. For the special case of manipulators with elastic joints,

[1]Department of Mechanical Engineering, Federal University of Rio Grande do Norte, Natal, Brazil
[2]Institute of Mechanics and Ocean Engineering, Hamburg University of Technology, Germany

Received: 9 July 2018; accepted: 7 January 2019

Corresponding author:
Wallace M. Bessa, Department of Mechanical Engineering, Federal University of Rio Grande do Norte, Campus Universitário Lagoa Nova, CEP 59072-970, Natal, RN, Brazil.
Email: wmbessa@ct.ufrn.br

Pervozvanski and Freidovich (1999) suggest criteria for choosing stabilizing PID gains.

Therefore, much effort has been made in order to improve both set-point regulation and trajectory tracking of underactuated mechanical systems. The most common strategies are controlled Lagrangians (Bloch et al., 2000, 2001), servo-constraint approaches (Blajer and Kołodziejczyk, 2007; Kovács and Bencsik, 2012; Bencsik et al., 2017; Otto and Seifried, 2018), backstepping (Chen and Huang, 2012; Xu and Hu, 2013; Rudra et al., 2014) and other passivity-based methods (Ortega et al., 2002; Gómez-Estern and der Schaft, 2004; Ryalat and Laila, 2016), as well as feedforward control by model inversion (Seifried, 2012a, 2012b) and input shaping (Singhose et al., 1994; Masoud and Daqaq, 2006; Maghsoudi et al., 2017), feedback linearization (Spong, 1994; Seifried, 2013), adaptive approaches (Nguyen and Dankowicz, 2015; Pucci et al., 2015), and sliding mode control (Ashrafiuon and Erwin, 2008; Xu and Özgüner, 2008; Qian et al., 2009; Sankaranarayanan and Mahindrakar, 2009; Muske et al., 2010).

The method of controlled Lagrangians uses the control input to customize the Lagrangian of the plant. Thereafter, energy methods can be used to inject damping into the system. Bloch et al. (2000, 2001) show that this approach can be used for the stabilization of some types of underactuated mechanical systems. By also using interconnection and damping assignment, Ortega et al. (2002) extend the method of controlled Lagrangians and apply it to the stabilization of a class of UMS with no physical damping. Gómez-Estern and der Schaft (2004) show that, under certain conditions, physical damping can also be taken into account without compromising passivity. Nevertheless, according to Liu and Yu (2013), passivity-based schemes have some limitations with respect to their practical application and are only applicable to systems with less than two relative degrees.

Trajectory tracking can be achieved by using an inverse model as feedforward control, which in turn is combined with a feedback controller. However, deriving the inverse model is usually not straightforward for nonlinear underactuated multibody systems. A numerical method for computing the inverse model has been proposed in Blajer and Kołodziejczyk (2004). It has been implemented and shown to be adequate for real-time applications in Otto (2016) and Otto and Seifried (2018). In Otto and Seifried (2018), the feedforward control based on the inverse model was augmented by a linear quadratic regulator (LQR)-based feedback loop to stabilize the tracking error.

Feedback linearization is a very common nonlinear control strategy, especially in the field of robotic manipulators, where it is also known as computed-torque (Slotine and Li, 1991). It is closely related to the inverse model approach and is shown to be applicable for underactuated systems in terms of partial feedback or input–output linearization (Spong, 1994). Nevertheless, feedback linearization in its basic form needs an accurate system model. Moreover, by applying partial feedback linearization, a thorough investigation of the internal dynamics, analyzed as zero dynamics, is necessary (Olfati-Saber, 2001).

Although several methods have been proposed in the last years, it should be highlighted that the control of uncertain UMS remains hard to be accomplished, especially if a high level of uncertainty is involved (Liu and Yu, 2013).

In general, model and parameter uncertainties can be handled by either robust or adaptive control schemes. In Pucci et al. (2015), for example, a collocated adaptive controller is proposed by extending the adaptive approach presented in Slotine and Weiping (1988) to the underactuated case. Nguyen and Dankowicz (2015) introduce an adaptive control scheme for underactuated robotic manipulators.

Sliding mode control is known to be one of the most successful approaches in handling bounded uncertainties (Shtessel et al., 2014). By means of a discontinuous law, perfect tracking on the sliding surface can theoretically be achieved. However, while the design of a stable sliding manifold is straightforward for fully actuated systems, this is not the case for underactuated ones. Ashrafiuon and Erwin (2008) propose a method based on the linearization of the model equations to derive stable sliding surfaces. Guo et al. (2014) also linearize the system dynamics about the equilibrium point, and then LQR-based and linear-matrix-inequality-based strategies are used to obtain the stabilizing manifold parameters. In Muske et al. (2010), an optimization scheme is used to derive the switching surface. An alternative method is proposed in Qian et al. (2009), where a hierarchical structure is adopted for the design of the stable manifold.

However, the discontinuous relay term in the sliding mode controller must be smoothed out to avoid the undesirable chattering effects. Although the adoption of properly designed boundary layers has proven effective in completely eliminating chattering, it leads to an inferior tracking performance notwithstanding. In this case, soft computing approaches may be used in order to improve the tracking performance (Yu and Kaynak, 2017).

Due to its ability to undertake assignments in an environment of imprecision and imperfect information, fuzzy logic has been widely employed to both identification and control of uncertain dynamical systems (Zadeh, 2008). Another important advantage of fuzzy logic is the capacity to deal with information described

in natural language (Zadeh, 1996). Hence, it allows human experience and knowledge to be expressed in an algorithmic manner, as well as incorporated into mathematically designed control laws.

On this basis, fuzzy logic has also been used to cope with uncertainties in the control of underactuated mechanical systems. Nakshatharan et al. (2015) use a fuzzy sliding surface for the stabilization of an underactuated ball and beam system driven by shape memory alloy actuators. In Yue et al. (2016), an adaptive fuzzy sliding mode controller is developed for a wheeled inverted pendulum. Li et al. (2014) design an adaptive fuzzy scheme based on the sliding mode method for underactuated mobile manipulators. Adaptive fuzzy sliding mode control has been also applied to the stabilization of an overhead container crane with two DOFs in Park et al. (2008). This approach is then extended for overhead cranes with three DOFs in Park et al. (2014).

In the special case of only one control input, that is, single-input–multiple-output (SIMO) systems, some different approaches have been proposed. In Zhang et al. (2014), for example, a self-organizing fuzzy algorithm is adopted to adjust the weighting matrix associated with the cost function of an optimal controller. Hwang et al. (2014) propose an adaptive fuzzy hierarchical sliding mode controller, where three distinct adaptive fuzzy inference systems should be adopted for each DOF. An adaptive fuzzy backstepping control scheme is also suggested by Azimi and Koofigar (2015).

For the more general problem of multiple-input–multiple-output (MIMO) underactuated mechanical systems, Wu et al. (2017) propose a robust approach by combining adaptive fuzzy inference systems with H_∞ control. In Wu et al. (2016), this control scheme is employed to reduce the sway motion of the payload in tower cranes.

In all aforementioned fuzzy schemes, either all error variables (Zhang et al., 2014; Nakshatharan et al., 2015) or all state variables (Park et al., 2008; Hwang et al., 2014; Li et al., 2014; Park et al., 2014; Azimi and Koofigar, 2015; Wu et al., 2016; Yue et al., 2016; Wu et al., 2017) are taken into account in the premises of the fuzzy rules. As a major drawback of this approach, as remarked by Bessa and Barrêto (2010) and Bessa et al. (2012), it can be asserted that the number of fuzzy sets and fuzzy rules becomes incredibly huge for large scale systems with several DOFs, which could compromise its applicability.

In this paper, an intelligent controller is proposed for MIMO underactuated mechanical systems subject to parameter uncertainties as well as unmodeled dynamics. The adopted approach is based on the sliding mode control to confer robustness against modeling inaccuracies and external disturbances, but an adaptive fuzzy inference system is embedded within the control law to improve set-point regulation and trajectory tracking. With the view to reduce the number of fuzzy sets and fuzzy rules, the switching variable, instead of all state variables, is considered in the premise of the related fuzzy rules. The convergence properties are demonstrated through a Lyapunov-like stability analysis. In order to illustrate the application of the intelligent controller and to evaluate its efficacy, the control law was implemented and tested in a 1:6 scale experimental container crane.

Thus, the following features of the proposed strategy can already be anticipated: (i) the ability to deal with a large class of MIMO underactuated systems; (ii) the robustness to parameter uncertainties, unmodeled dynamics, and external disturbances; (iii) the necessity of only one fuzzy inference system per control input; and (iv) the adoption of a single variable in the premise of the fuzzy rules. The last two features not only simplify the design process and the resulting control law, but also reduce the required computational time. These attributes, when combined with the first two, allow for the intelligent controller to be straightforwardly implemented in industrial and real-world applications.

As a general objective of this paper, it is shown that soft computing techniques can be easily associated with already available control methods for underactuated systems, in order to enhance the overall system performance.

Hence, a sliding mode approach defined in Ashrafiuon and Erwin (2008) is briefly reviewed in Section 2. This sliding mode controller is then used as a basis for the intelligent strategy proposed in Section 3. Finally, by means of experimental results, both control schemes are compared in Section 4, and the concluding remarks are presented in Section 5.

2. Sliding mode control

The equations of motion of a mechanical system with n DOFs and m actuator inputs are usually expressed in the following vector form (Seifried, 2013)

$$M(\boldsymbol{q})\ddot{\boldsymbol{q}} + \boldsymbol{k}(\boldsymbol{q}, \dot{\boldsymbol{q}}) = \boldsymbol{g}(\boldsymbol{q}, \dot{\boldsymbol{q}}) + \boldsymbol{B}(\boldsymbol{q})\boldsymbol{u} \tag{1}$$

where $\boldsymbol{q} \in \mathbb{R}^n$ is the vector of generalized coordinates, $\boldsymbol{u} \in \mathbb{R}^m$ the actuator input vector, $\boldsymbol{M}(\boldsymbol{q}) \in \mathbb{R}^{n\times n}$ is the positive definite and symmetric inertia matrix, $\boldsymbol{k}(\boldsymbol{q}, \dot{\boldsymbol{q}}) \in \mathbb{R}^n$ takes the Coriolis and centrifugal effects into account, $\boldsymbol{g}(\boldsymbol{q}, \dot{\boldsymbol{q}}) \in \mathbb{R}^n$ represents the generalized applied forces, and $\boldsymbol{B}(\boldsymbol{q}) \in \mathbb{R}^{n\times m}$ is the input matrix.

Remark 1. *The mechanical system described in equation (1) is called fully-actuated if* $m = \mathrm{rank}(\boldsymbol{B}) = n$, *or underactuated if* $m = \mathrm{rank}(\boldsymbol{B}) < n$.

Now, considering an underactuated mechanical system, the vector of generalized coordinates can be partitioned as $\boldsymbol{q} = [\boldsymbol{q}_a^\top \ \boldsymbol{q}_u^\top]^\top$, where $\boldsymbol{q}_a \in \mathbb{R}^m$ and $\boldsymbol{q}_u \in \mathbb{R}^{n-m}$ denote, respectively, actuated and unactuated coordinates. Without loss of generality, the input matrix can be also conveniently assumed to be $\boldsymbol{B}(\boldsymbol{q}) = [\boldsymbol{I}_m \ \boldsymbol{0}^\top]^\top$, where $\boldsymbol{I}_m$ is the $m \times m$ identity matrix, and $\boldsymbol{0}$ is the $(n-m) \times m$ zero matrix. Hence, equation (1) may be rewritten as

$$\begin{bmatrix} \boldsymbol{M}_{aa} & \boldsymbol{M}_{au} \\ \boldsymbol{M}_{au}^\top & \boldsymbol{M}_{uu} \end{bmatrix} \begin{bmatrix} \ddot{\boldsymbol{q}}_a \\ \ddot{\boldsymbol{q}}_u \end{bmatrix} = \begin{bmatrix} \boldsymbol{f}_a + \boldsymbol{u} \\ \boldsymbol{f}_u \end{bmatrix} \tag{2}$$

where $\boldsymbol{f}_a = \boldsymbol{g}_a - \boldsymbol{k}_a$ and $\boldsymbol{f}_u = \boldsymbol{g}_u - \boldsymbol{k}_u$.

Then, in order to develop a sliding mode controller, Ashrafiuon and Erwin (2008) propose to solve equation (2) for the accelerations

$$\ddot{\boldsymbol{q}}_a = \boldsymbol{M}_{aa}'^{-1}(\boldsymbol{f}_a' + \boldsymbol{u}) \tag{3a}$$

$$\ddot{\boldsymbol{q}}_u = \boldsymbol{M}_{uu}'^{-1}(\boldsymbol{f}_u' - \boldsymbol{M}_{au}^\top \boldsymbol{M}_{aa}^{-1}\boldsymbol{u}) \tag{3b}$$

where $\boldsymbol{M}_{aa}' = \boldsymbol{M}_{aa} - \boldsymbol{M}_{au}\boldsymbol{M}_{uu}^{-1}\boldsymbol{M}_{au}^\top$, $\boldsymbol{M}_{uu}' = \boldsymbol{M}_{uu} - \boldsymbol{M}_{au}^\top \boldsymbol{M}_{aa}^{-1}\boldsymbol{M}_{au}$, $\boldsymbol{f}_a' = \boldsymbol{f}_a - \boldsymbol{M}_{au}\boldsymbol{M}_{uu}^{-1}\boldsymbol{f}_u$, and $\boldsymbol{f}_u' = \boldsymbol{f}_u - \boldsymbol{M}_{au}^\top \boldsymbol{M}_{aa}^{-1}\boldsymbol{f}_a$.

Hence, by defining $\tilde{\boldsymbol{q}} = \boldsymbol{q} - \boldsymbol{q}^d$ as the tracking error vector, a sliding manifold can be established in the state space by the equation $\boldsymbol{s}(\tilde{\boldsymbol{q}}) = \boldsymbol{0}$, with $\boldsymbol{s}(\tilde{\boldsymbol{q}}) : \mathbb{R}^n \to \mathbb{R}^m$ defined as a weighted combination of both position and velocity tracking error (Ashrafiuon and Erwin, 2008)

$$\begin{aligned} \boldsymbol{s} &= \boldsymbol{\alpha}_a \dot{\tilde{\boldsymbol{q}}}_a + \boldsymbol{\lambda}_a \tilde{\boldsymbol{q}}_a + \boldsymbol{\alpha}_u \dot{\tilde{\boldsymbol{q}}}_u + \boldsymbol{\lambda}_u \tilde{\boldsymbol{q}}_u \\ &= \boldsymbol{\alpha}_a \dot{\boldsymbol{q}}_a + \boldsymbol{\alpha}_u \dot{\boldsymbol{q}}_u + \boldsymbol{s}_r \end{aligned} \tag{4}$$

with $\boldsymbol{s}_r = -\boldsymbol{\alpha}_a \dot{\boldsymbol{q}}_a^d + \boldsymbol{\alpha}_u \dot{\boldsymbol{q}}_u^d + \boldsymbol{\lambda}_a \tilde{\boldsymbol{q}}_a + \boldsymbol{\lambda}_u \tilde{\boldsymbol{q}}_u$, and constant matrices $\boldsymbol{\alpha}_a \in \mathbb{R}^{m \times m}$, $\boldsymbol{\lambda}_a \in \mathbb{R}^{m \times m}$, $\boldsymbol{\alpha}_u \in \mathbb{R}^{m \times (n-m)}$, and $\boldsymbol{\lambda}_u \in \mathbb{R}^{m \times (n-m)}$.

On this basis, following Ashrafiuon and Erwin (2008), the sliding mode controller is defined as

$$\boldsymbol{u} = -\hat{\boldsymbol{M}}_s^{-1}[\hat{\boldsymbol{f}}_s + \dot{\boldsymbol{s}}_r + \boldsymbol{\kappa}\mathrm{sgn}(\boldsymbol{s})] \tag{5}$$

where $\hat{\boldsymbol{M}}_s$ and $\hat{\boldsymbol{f}}_s$ are estimates of $\boldsymbol{M}_s = \boldsymbol{\alpha}_a \boldsymbol{M}_{aa}'^{-1} - \boldsymbol{\alpha}_u \boldsymbol{M}_{uu}'^{-1} \boldsymbol{M}_{au}^\top \boldsymbol{M}_{aa}^{-1}$ and $\boldsymbol{f}_s = \boldsymbol{\alpha}_a \boldsymbol{M}_{aa}'^{-1} \boldsymbol{f}_a' - \boldsymbol{\alpha}_u \boldsymbol{M}_{uu}'^{-1} \boldsymbol{f}_u'$, respectively, and

$$\boldsymbol{\kappa}\,\mathrm{sgn}(\boldsymbol{s}) = [\kappa_1 \,\mathrm{sgn}(s_1) \ \ldots \ \kappa_m \,\mathrm{sgn}(s_m)]^\top \tag{6}$$

with the control gain $\boldsymbol{\kappa}$ defined with respect to the bounds of $\boldsymbol{f}_s$.

For more details about the stability analysis of the sliding mode controller defined in equation (5) the reader is referred to Ashrafiuon and Erwin (2008).

3. Adaptive fuzzy sliding mode control

Conventional controllers frequently rely on an accurate model of the plant, which in general is very difficult to achieve. Even in the case of sliding modes, the discontinuous relay term in the control law has to be smoothed out in order to avoid the undesirable chattering effects. However, despite its capacity to reduce chattering, the adoption of a boundary layer leads to an inferior tracking performance, which is even more worrying in the case of systems subject to a high degree of uncertainty. In order to overcome these handicaps, computational intelligence may be conveniently combined with sliding modes, leading to a robust intelligent control approach.

According to Antsaklis (2001), intelligent controllers should emulate important characteristics of human intelligence. In this context, among other attributes, an intelligent controller must at least be able to: (i) incorporate some prior knowledge about the plant, in order to make reasonable predictions about the expected dynamic behavior; (ii) adapt itself to changes in the plant and in the environment; and (iii) learn by experience as well as acquire knowledge by interacting with the environment, to improve the capacity to predict plant dynamics. Also, it is worth noting that, depending on application requirements, the controller should be robust to external disturbances, with the view to ensure safe operating conditions.

Thus, in order to comply with prediction and robustness issues, here a sliding mode approach is adopted. As a matter of fact, any model-based controller is able to predict to some extent the dynamics of the plant, but the robustness of the sliding mode method is a really attractive feature. In addition, fuzzy logic is chosen in this work to fulfill the adaptation and learning attributes. On this basis, an adaptive fuzzy inference system is embedded in the sliding mode controller to learn about the actual dynamic behavior of the plant and to compensate for the unmodeled effects.

Therefore, in the following only a partial knowledge about the mechanical system in equation (1) is considered. In this case, uncertainties concerning the inertia matrix, $\Delta\boldsymbol{M}$, and applied forces, $\Delta\boldsymbol{f}$, as well as eventual external perturbations $\boldsymbol{\varepsilon}$ are also taken into account

$$(\boldsymbol{M} + \Delta\boldsymbol{M})\ddot{\boldsymbol{q}} = \boldsymbol{f} + \Delta\boldsymbol{f} + \boldsymbol{u} + \boldsymbol{\varepsilon} \tag{7}$$

For simplicity reasons, all uncertainties and external perturbations in equation (7) are now enclosed in a new disturbance vector $\boldsymbol{d} = \boldsymbol{\varepsilon} + \Delta\boldsymbol{f} - \Delta\boldsymbol{M}\ddot{\boldsymbol{q}}$. Also, for control purposes, this vector is partitioned as $\boldsymbol{d} = [\boldsymbol{d}_a^\top \ \boldsymbol{d}_u^\top]^\top$.

Now, following Ashrafiuon and Erwin (2008), the new uncertain underactuated mechanical system can be solved for the accelerations

$$\ddot{\boldsymbol{q}}_a = \boldsymbol{M}'^{-1}_{aa}(\boldsymbol{f}'_a + \boldsymbol{u} + \boldsymbol{d}'_a) \tag{8a}$$

$$\ddot{\boldsymbol{q}}_u = \boldsymbol{M}'^{-1}_{uu}(\boldsymbol{f}'_u - \boldsymbol{M}^{\top}_{au}\boldsymbol{M}^{-1}_{aa}\boldsymbol{u} + \boldsymbol{d}'_u) \tag{8b}$$

with $\boldsymbol{M}'_{aa}$, $\boldsymbol{M}'_{uu}$, $\boldsymbol{f}'_a$, and $\boldsymbol{f}'_u$ defined as before, and $\boldsymbol{d}'_a = \boldsymbol{d}_a - \boldsymbol{M}_{au}\boldsymbol{M}^{-1}_{uu}\boldsymbol{d}_u$, and $\boldsymbol{d}'_u = \boldsymbol{d}_u - \boldsymbol{M}^{\top}_{au}\boldsymbol{M}^{-1}_{aa}\boldsymbol{d}_a$. Also, a combined disturbance vector can be stated as $\boldsymbol{d}_s = \boldsymbol{\alpha}_a\boldsymbol{M}'^{-1}_{aa}\boldsymbol{d}'_a - \boldsymbol{\alpha}_u\boldsymbol{M}'^{-1}_{uu}\boldsymbol{d}'_u$.

At this point, regarding the development of the control law, the following assumptions should yet be made:

Assumption 1. *The inertia matrix $\boldsymbol{M}$ is symmetric, bounded, and positive definite for any bounded $\boldsymbol{q}$.*

Assumption 2. *The vector of disturbances $\boldsymbol{d}$ is unknown but bounded.*

Assumption 3. *The vector of generalized coordinates $\boldsymbol{q}$ is available.*

Assumption 4. *The desired trajectory $\boldsymbol{q}^d$ is once differentiable with respect to time. Furthermore, every component of $\boldsymbol{q}^d$ is available and with known bounds.*

Remark 2. *From Assumptions 1 and 2, it can be clearly ascertained that $\boldsymbol{d}'_a$ and $\boldsymbol{d}'_u$ are bounded. Since $\boldsymbol{\alpha}_a$ and $\boldsymbol{\alpha}_u$ are chosen by the designer of the control law, it can also be inferred from these assumptions that $\boldsymbol{d}_s$ is bounded.*

Assumption 1 as well as Assumptions 2–4 are standard premises in the fields of multibody systems (Slotine and Li, 1991; Spong et al., 2005) and sliding mode control (Utkin, 1992), respectively. Moreover, due to its adaptive feature, the proposed intelligent controller can still deal with uncertainties in underactuated mechanical systems, even if Assumption 2 is not taken into account. However, this premise is required if, beyond convergence and stability, also robustness with respect to the considered bounds is to be claimed.

Thus, we propose the adoption of an intelligent compensator $\hat{\boldsymbol{d}}$ to cope with the uncertainties and external disturbances related to $\boldsymbol{d}_s$. For each component $\hat{d}_i$, a zero order Takagi–Sugeno–Kang (TSK) inference system (Jang et al., 1997) is established. The associated fuzzy rules can be stated in a linguistic manner as follows

$$\textit{If } s_i \quad \textit{is } S_{ij}, \quad \textit{then } \hat{d}_{ij} = \hat{D}_{ij}; \quad j = 1, 2, \ldots, N$$

where S_{ij} are fuzzy sets, whose membership functions could be properly chosen.

Considering that the rules define numerical values as output $\hat{D}_{ij}$, the final output of each $\hat{d}$ can be computed by a weighted average

$$\hat{d}_i(s_i) = \hat{\boldsymbol{D}}_i^{\top}\Psi_i(s_i) \tag{9}$$

where $\hat{\boldsymbol{D}}_i = [\hat{D}_{i1} \ \ldots \ \hat{D}_{iN}]^{\top}$ are vectors containing the attributed values $\hat{D}_{ij}$ to the fuzzy rules, $\Psi_i(s_i) = [\psi_{i1}(s_i) \ \ldots \ \psi_{iN}(s_i)]^{\top}$, with $\psi_{ij}(s_i) = w_{ij}/\sum_{j=1}^{N} w_{ij}$, and w_{ij} is the firing strength of each rule.

In order to ensure the best possible estimate, let the vector of adjustable parameters be automatically updated by the following adaptation law

$$\dot{\hat{\boldsymbol{D}}}_i = \varphi_i s_i \Psi_i(s_i) \tag{10}$$

where φ_i are strictly positive constants related to the adaptation rate. In order to avoid unnecessary overshoots, the adaptation law may be activated as soon as the sliding variable reaches the boundary layer.

Remark 3. *Considering that fuzzy logic can perform universal approximation (Kosko, 1994), the output of the TSK inference systems can approximate $\boldsymbol{d}_s$ to an arbitrary degree of accuracy $\boldsymbol{\delta} = \hat{\boldsymbol{d}}^* - \boldsymbol{d}_s$, where $\hat{\boldsymbol{d}}^*$ is the output related to set of optimal parameter vectors $\hat{\boldsymbol{D}}_i^*$.*

Therefore, the intelligent compensator can be added to the sliding mode controller as follows

$$\boldsymbol{u} = -\hat{\boldsymbol{M}}_s^{-1}[\hat{\boldsymbol{f}}_s + \hat{\boldsymbol{d}} + \dot{\boldsymbol{s}}_r + \boldsymbol{\kappa}\,\mathrm{sgn}(\boldsymbol{s})] \tag{11}$$

where the components of $\boldsymbol{\kappa} \in \mathbb{R}^m$ are defined according to $\kappa_i \geq \eta + \delta_i + |\hat{d}_i|$, and η is a strictly positive constant related to the reaching time.

It should be highlighted that the adoption of a single variable on the premise of the fuzzy rules allows the reduction of computational complexity. In fact, if either n generalized coordinates $\boldsymbol{q}$ or n tracking errors $\tilde{\boldsymbol{q}}$ have been adopted as inputs, instead of the sliding variables, the number of fuzzy rules and the adaptive laws that have to be integrated at each time step would exponentially grow from m to m^n. Keeping computational complexity low makes the online compensation scheme suitable for real-time implementations. The main idea behind this approach relies on a well-known feature of sliding mode control: the convergence to the sliding surface implies exponential convergence of the tracking error to zero.

Moreover, the adoption of s_i as input to each fuzzy inference system also facilitates the design of the fuzzy rules. In this case, the universe of discourse remains one-dimensional and limited by the width of the boundary layer. Hence, the related fuzzy sets can be either homogeneously spread over the domain or heuristically

concentrated in the vicinity of the sliding manifold in order to allow fine tuning. On this basis, since the output of each rule is automatically set by equation (10), the fuzzy inference system can be easily attained.

In addition, it should be highlighted that this procedure has already been successfully applied to the dynamic positioning of remotely operated vehicles (Bessa et al., 2008, 2010), vibration suppression in smart structures (Bessa et al., 2013), tracking of unstable periodic orbits in a chaotic pendulum (Bessa et al., 2014), and depth regulation of a diving cell (Bessa et al., 2015).

Now, considering that the adopted sliding surface is a stable manifold (Ashrafiuon and Erwin, 2008), we just have to prove its attractiveness, in order to ensure exponential convergence and stability of the proposed controller (Slotine and Li, 1991; Khalil, 2001). On this account, the attractiveness of the sliding manifold is proven in the following theorem.

Theorem 1. *Consider the uncertain underactuated mechanical system equation (8) subject to Assumptions 1–4. Then, the controller defined by equations (9), (10), and (11) ensures the convergence of the tracking errors to the sliding manifold* $\boldsymbol{s}(\tilde{\boldsymbol{q}}) = 0$.

Proof. Let a positive-definite function V_1 be defined as

$$V_1(t) = \frac{1}{2}\boldsymbol{s}^\top \boldsymbol{s} + \sum_{i=1}^{m} \frac{1}{2\varphi_i} \Delta_i^\top \Delta_i \tag{12}$$

where $\Delta_i = \hat{\boldsymbol{D}}_i - \hat{\boldsymbol{D}}_i^*$. Thus, the time derivative of V_1 is

$$\begin{aligned}
\dot{V}_1(t) &= \boldsymbol{s}^\top \dot{\boldsymbol{s}} + \sum_{i=1}^{m} \varphi_i^{-1} \Delta_i^\top \dot{\Delta}_i \\
&= \boldsymbol{s}^\top (\boldsymbol{\alpha}_a \ddot{\boldsymbol{q}}_a + \boldsymbol{\alpha}_u \ddot{\boldsymbol{q}}_u + \dot{\boldsymbol{s}}_r) + \sum_{i=1}^{m} \varphi_i^{-1} \Delta_i^\top \dot{\Delta}_i \\
&= \boldsymbol{s}^\top [\boldsymbol{\alpha}_a \boldsymbol{M}'^{-1}_{aa} (\boldsymbol{f}'_a + \boldsymbol{u} + \boldsymbol{d}'_a) + \\
&\quad + \boldsymbol{\alpha}_u \boldsymbol{M}'^{-1}_{uu} (\boldsymbol{f}'_u - \boldsymbol{M}'^{\top}_{au} \boldsymbol{M}'^{-1}_{aa} \boldsymbol{u} + \boldsymbol{d}'_u) + \dot{\boldsymbol{s}}_r] + \\
&\quad + \sum_{i=1}^{m} \varphi_i^{-1} \Delta_i^\top \Delta_i \\
&= \boldsymbol{s}^\top [\boldsymbol{f}_s + \boldsymbol{d}_s + \dot{\boldsymbol{s}}_r + \boldsymbol{M}_s \boldsymbol{u}] + \sum_{i=1}^{m} \varphi_i^{-1} \Delta_i^\top \dot{\Delta}_i
\end{aligned}$$

Thus, applying the control law equation (11), recalling Remark 3, and noting that $\dot{\Delta}_i = \dot{\hat{\boldsymbol{D}}}_i$, $\dot{V}_1$ becomes

$$\begin{aligned}
\dot{V}_1(t) &= -\boldsymbol{s}^\top [\hat{\boldsymbol{d}} - \hat{\boldsymbol{d}}^* + \boldsymbol{\delta} + \boldsymbol{\kappa}\,\mathrm{sgn}(\boldsymbol{s})] + \sum_{i=1}^{m} \varphi_i^{-1} \Delta_i^\top \dot{\hat{\boldsymbol{D}}}_i \\
&= -\boldsymbol{s}^\top [\boldsymbol{\delta} + \boldsymbol{\kappa}\,\mathrm{sgn}(\boldsymbol{s})] \\
&\quad + \sum_{i=1}^{m} \varphi_i^{-1} \Delta_i^\top [\dot{\hat{\boldsymbol{D}}}_i - \varphi_i s_i \Psi_i(s_i)]
\end{aligned}$$

Hence, considering that $\kappa_i \geq \eta + \delta_i + |\hat{d}_i|$, and defining $\hat{\boldsymbol{D}}_i$ according to equation (10), one obtains

$$\dot{V}_1(t) \leq -\eta ||\boldsymbol{s}||_1 \tag{13}$$

This implies $V_1(t) \leq V_1(0)$ and that $\boldsymbol{s}$ as well as every Δ_i are bounded. From equation (4), it can be verified that $\tilde{\boldsymbol{q}}$ is also bounded. Thereby, Assumption 4 implies that $\dot{\boldsymbol{s}}$ is also bounded, which in fact also guarantees the uniform continuity of $\boldsymbol{s}$ (Slotine and Li, 1991).

Integrating both sides of equation (13) shows that

$$\lim_{t\to\infty} \int_0^t \eta ||\boldsymbol{s}||_1 \,\mathrm{d}\tau \leq \lim_{t\to\infty} [V_1(0) - V_1(t)] \leq V_1(0) < \infty$$

Therefore, considering that $\boldsymbol{s}$ is uniformly continuous, it follows from Barbalat's lemma (Hou et al., 2010) that $\boldsymbol{s} \to 0$ as $t \to \infty$, which ensures the convergence of the tracking errors to the sliding manifold and completes the proof. □

However, it should be noted that the presence of a discontinuous term, $\boldsymbol{\kappa}\,\mathrm{sgn}(\boldsymbol{s})$, in the control law leads to the well-known chattering effect. Particularly in the case of mechanical systems, this high-frequency oscillation in the controlled variable should be avoided, since it can excite unmodeled vibration modes. In order to overcome this issue, thin boundary layers in the neighborhood of the sliding surfaces can be defined by replacing the sign function by a smooth approximation of it

$$\boldsymbol{u} = -\hat{\boldsymbol{M}}_s^{-1} [\hat{\boldsymbol{f}}_s + \hat{\boldsymbol{d}} + \dot{\boldsymbol{s}}_r + \boldsymbol{\kappa}\,\mathrm{sat}(\phi^{-1}\boldsymbol{s})] \tag{14}$$

Hereby, $\phi \in \mathbb{R}^{m\times m}$ is a diagonal matrix with m positive entries ϕ_i, and $\mathrm{sat}(\cdot)$ is the saturation function

$$\mathrm{sat}(s_i/\phi_i) = \begin{cases} \mathrm{sgn}(s_i) & \text{if} \quad |s_i/\phi_i| \geq 1 \\ s_i/\phi_i & \text{if} \quad |s_i/\phi_i| < 1 \end{cases} \tag{15}$$

Finally, Theorem 2 shows that the smooth intelligent controller, equation (14), ensures the convergence of the tracking error to the invariant set defined by the boundary layers. As discussed by Bessa (2009), this is a sufficient condition to ensure the convergence of the tracking error to a bounded region, as well as the stability of the controlled system.

Theorem 2. *Consider the uncertain underactuated mechanical system equation (8) subject to Assumptions 1–4. Then, the controller defined by equations (9), (10), and (14) ensures the convergence of the tracking errors to the manifold* $\Phi = \{\tilde{\boldsymbol{q}} \in \mathbb{R}^n \mid |s_i| \leq \phi_i, i = 1, \ldots, m\}$.

Proof. Let a positive-definite Lyapunov function candidate V_2 be defined as

$$V_2(t) = \frac{1}{2}\boldsymbol{s}_\phi^\top \boldsymbol{s}_\phi \tag{16}$$

where each component of $\boldsymbol{s}_\phi(\tilde{\boldsymbol{q}})$ is a measure of the distance between s_i and its related boundary layer, and is computed as follows

$$\boldsymbol{s}_\phi(\tilde{\boldsymbol{q}}) = \boldsymbol{s} - \phi \mathrm{sat}(\phi^{-1}\boldsymbol{s}) \tag{17}$$

Noting that $\dot{\boldsymbol{s}}_\phi = \boldsymbol{s}_\phi = 0$ inside Φ, and $\dot{\boldsymbol{s}}_\phi = \dot{\boldsymbol{s}}$ outside of it, then the time derivative of V_2 becomes

$$\begin{aligned}\dot{V}_2(t) &= \boldsymbol{s}_\phi^\top \dot{\boldsymbol{s}} = \boldsymbol{s}_\phi^\top(\boldsymbol{\alpha}_a \ddot{\boldsymbol{q}}_a + \boldsymbol{\alpha}_u \ddot{\boldsymbol{q}}_u + \dot{\boldsymbol{s}}_r) \\ &= \boldsymbol{s}_\phi^\top[\boldsymbol{\alpha}_a \boldsymbol{M}_{aa}'^{-1}(\boldsymbol{f}_a' + \boldsymbol{u} + \boldsymbol{d}_a') + \\ &\quad + \boldsymbol{\alpha}_u \boldsymbol{M}_{uu}'^{-1}(\boldsymbol{f}_u' - \boldsymbol{M}_{au}^\top \boldsymbol{M}_{aa}^{-1}\boldsymbol{u} + \boldsymbol{d}_u') + \dot{\boldsymbol{s}}_r] \\ &= \boldsymbol{s}_\phi^\top[\boldsymbol{f}_s + \boldsymbol{d}_s + \dot{\boldsymbol{s}}_r + \boldsymbol{M}_s \boldsymbol{u}]\end{aligned}$$

Thereby, applying the control law equation (14), and noting that $\mathrm{sat}(\phi^{-1}\boldsymbol{s}) = \mathrm{sgn}(\boldsymbol{s}_\phi)$ outside Φ and $|\hat{d}_i - \hat{d}_i^*| \le |\hat{d}_i|$, one obtains

$$\begin{aligned}\dot{V}_2(t) &= -\boldsymbol{s}_\phi^\top[\hat{\boldsymbol{d}} - \hat{\boldsymbol{d}}^* + \boldsymbol{\delta} + \boldsymbol{\kappa}\mathrm{sgn}(\boldsymbol{s}_\phi)] \\ &\le -\eta ||\boldsymbol{s}_\phi||_1\end{aligned} \tag{18}$$

This implies $V_2(t) \le V_2(0)$ and that $\boldsymbol{s}_\phi$ is bounded. From Theorem 1, as well as equations (4) and (17), it can be verified that $\tilde{\boldsymbol{q}}$ remains bounded. Hence, by noting that $\dot{\boldsymbol{s}}_\phi$ is limited by $\dot{\boldsymbol{s}}$, it follows from Theorem 1 that $\dot{\boldsymbol{s}}_\phi$ is also bounded, which guarantees its uniform continuity.

Integrating both sides of equation (18) shows that

$$\lim_{t\to\infty} \int_0^t \eta ||\boldsymbol{s}_\phi||_1 \, \mathrm{d}\tau \le \lim_{t\to\infty}[V_2(0) - V_2(t)] \le V_2(0) < \infty$$

Thus, since $\boldsymbol{s}_\phi$ is uniformly continuous, Barbalat's lemma (Hou et al., 2010) is evoked to show that $\boldsymbol{s}_\phi \to \boldsymbol{0}$ and $\tilde{\boldsymbol{q}} \to \Phi$ as $t \to \infty$, which ensures the boundedness of all closed-loop signals and the asymptotical stability of Φ. □

4. Experimental results

The proposed intelligent controller is now evaluated in an experimental overhead container crane, available at the Institute of Mechanics and Ocean Engineering at Hamburg University of Technology, as shown in Figure 1. The experimental setup consists of a trolley with a motion range of 13 m, and a 1:6 scale container with 0.35m × 0.37m × 0.86m that is attached to the trolley by four cables. The cables are synchronously actuated, and their length can be varied within 9 m. Both trolley position and cable lengths are measured by absolute angular encoders, and can be directly actuated. The swing angle, on the other hand, is an unactuated variable, and is estimated from the measured forces on the cables, using an unscented Kalman filter (Kreuzer et al., 2012).

Figure 1. Experimental crane at the Institute of Mechanics and Ocean Engineering.

In order to develop the control law, a simple mathematical model of the overhead container crane, is considered

$$\begin{aligned}&\begin{bmatrix} M+m & m\sin\theta & ml\cos\theta \\ m\sin\theta & m & 0 \\ ml\cos\theta & 0 & ml^2 \end{bmatrix}\begin{bmatrix} \ddot{x} \\ \ddot{l} \\ \ddot{\theta} \end{bmatrix} \\ &= \begin{bmatrix} m\dot{\theta}(\dot{\theta}l\sin\theta - 2\dot{l}\cos\theta) \\ m(l\dot{\theta}^2 + g\cos\theta) \\ -ml(2\dot{l}\dot{\theta} + g\sin\theta) \end{bmatrix} + \begin{bmatrix} u_x \\ u_l \\ 0 \end{bmatrix}\end{aligned} \tag{19}$$

where u_x and u_l are, respectively, the control forces acting on the trolley and the cables, x is the trolley position, l stands for the length of the cables, θ represents the swing angle, M is the mass of the trolley, and m is the container mass. Thus, the vectors with actuated and unactuated variables are $\boldsymbol{q}_a = [x\ l]^\top$ and $\boldsymbol{q}_u = [\theta]$, respectively.

It should be noted, however, that no friction, damping force or actuator dynamics are incorporated into the mathematical model described in equation (19). Unlike the inertial effects considered in the model, friction and damping are not so easy to be accurately represented. Also, the dynamics of powertrain would require experimental research in order to obtain the proper model and its parameters. Although certainly

present in the experimental setup, these effects are not taken into account in the development of the control law to demonstrate the robustness of the proposed scheme against unmodeled dynamics.

Both trolley and container masses are also considered as uncertain. Their nominal values are actually well-known (270 kg and 12.9 kg, respectively), but uncertainties of $\pm 70\%$ over the container mass and $\pm 40\%$ over the mass of the trolley are deliberately assumed, in order to show that the controller is also robust to large parametric variations.

Concerning the assumptions made in the development of the controller (see Section 3), it is worth noting that they are rigorously met by the testbench conditions. Assumption 2 is valid for the considered system, as can be verified by direct inspection of equation (19) and the aforementioned values. Assumption 2 is reasonable, since the related disturbances include uncertainties with respect to the inertia matrix and friction issues. All these effects are bounded due to either physical limitations or finite energy supply. Assumption 3 is always required for the design of state feedback controllers and is also valid here, since all states are either measurable or observable. Lastly, Assumption 4 is plausible, since the state trajectory can be arbitrarily chosen to be four times continuously differentiable, which is also used here. Moreover, even in a hypothetical case, where the desired trajectory is not continuously differentiable, it is well known that a first-order low pass filter could be used to define $\boldsymbol{q}^d$ (Farrell and Polycarpou, 2006).

The efficacy and robustness of the intelligent controller is then evaluated for both stabilization and tracking problems. It should be highlighted that the experimental container crane must be controlled by means of reference velocities, and not forces, due to the requirements of the actuators. Therefore, the computed control efforts (u_x and u_l) are converted to the required velocity values (v_x and v_l) at each time step through the integration of equation (8a), with the unknown disturbance set to zero: $\boldsymbol{d}'_a = 0$.

4.1. Stabilization of the swing angle

A series of 47 experiments has been conducted to investigate the influence of the controller parameters on the stabilization of the unactuated variable, namely, the swing angle, considering both the here developed intelligent sliding mode controller (ISMC) as well as the conventional scheme (SMC) from Section 2. After each trial, the container swing was damped completely and the unscented Kalman filter was initialized, in order to ensure equal initial conditions and to guarantee that the swing angle is correctly estimated. In all experiments, the container is set to swing by imposing for 3 seconds a constant velocity $v_x = -0.5$ m/s to the trolley. Then, after a waiting period, the controller is turned on at $t = 10$ seconds with the aim to reduce the swing amplitude.

Table 1. Experiments and corresponding parameters.

Experiment number	$\phi_{1,2}$	$\delta_{1,2}$	$\varphi_{1,2}$	M	m
1	–	1	0	270 kg	12.9 kg
2	–	2	0	270 kg	12.9 kg
$3_{a,b,c,d,e}$	1	1	0	$\in$ [170 370] kg	$\in$ [3.9 21.9] kg
$4_{a,b,c,d,e}$	1	2	0	$\in$ [170 370] kg	$\in$ [3.9 21.9] kg
$5_{a,b,c,d,e}$	5	1	0	$\in$ [170 370] kg	$\in$ [3.9 21.9] kg
$6_{a,b,c,d,e}$	5	2	0	$\in$ [170 370] kg	$\in$ [3.9 21.9] kg
$7_{a,b,c,d,e}$	1	1	50	$\in$ [170 370] kg	$\in$ [3.9 21.9] kg
$8_{a,b,c,d,e}$	1	2	50	$\in$ [170 370] kg	$\in$ [3.9 21.9] kg
$9_{a,b,c,d,e}$	5	1	50	$\in$ [170 370] kg	$\in$ [3.9 21.9] kg
$10_{a,b,c,d,e}$	5	2	50	$\in$ [170 370] kg	$\in$ [3.9 21.9] kg
11	5	1	0	370 kg	3.9 kg
12	5	1	25	370 kg	3.9 kg
13	5	1	50	370 kg	3.9 kg
14	5	1	75	370 kg	3.9 kg
15	5	1	100	370 kg	3.9 kg

For simplification, the control parameters ϕ_i, δ_i, and φ_i are chosen to be equal for both components u_x and u_l. It is also worth noting that the ISMC can be easily converted to the conventional SMC by setting the vectors with the output of the fuzzy rules and the adaptation rates to zero, that is, $\hat{\boldsymbol{D}}_i = 0$ and $\varphi_i = 0$. An overview of the control parameters considered in each experiment is summarized in Table 1. Here, it is also important to note that $\varphi_{1,2} = 0$ refer to SMC while $\varphi_{1,2} \neq 0$ refer to the ISMC.

The first two experiments are related to the conventional sliding mode approach, that is, with sgn($\boldsymbol{s}$) in the control law. The aim of these first trials is to show the occurrence of chattering in this context. The masses of both container and trolley are considered perfectly known, and the influence of two different values for $\delta_{1,2}$ is evaluated, $\delta_{1,2} = 1$ and $\delta_{1,2} = 2$. The other chosen parameters are: $\eta = 0.01$,

$$\boldsymbol{\alpha}_a = \begin{bmatrix} 1 & 0 \\ 0 & 1 \end{bmatrix}, \quad \boldsymbol{\alpha}_u = \begin{bmatrix} 1.5 \\ 0 \end{bmatrix},$$
$$\boldsymbol{\lambda}_a = \begin{bmatrix} 0.5 & 0 \\ 0 & 0.5 \end{bmatrix}, \quad \boldsymbol{\lambda}_u = \begin{bmatrix} -5 \\ 0 \end{bmatrix}$$

Figure 2 shows the results obtained in experiment #2 using SMC with sgn($\boldsymbol{s}$). Since the results related to experiment #1 are closely similar to those from experiment #2, they are not detailed here. The overall control

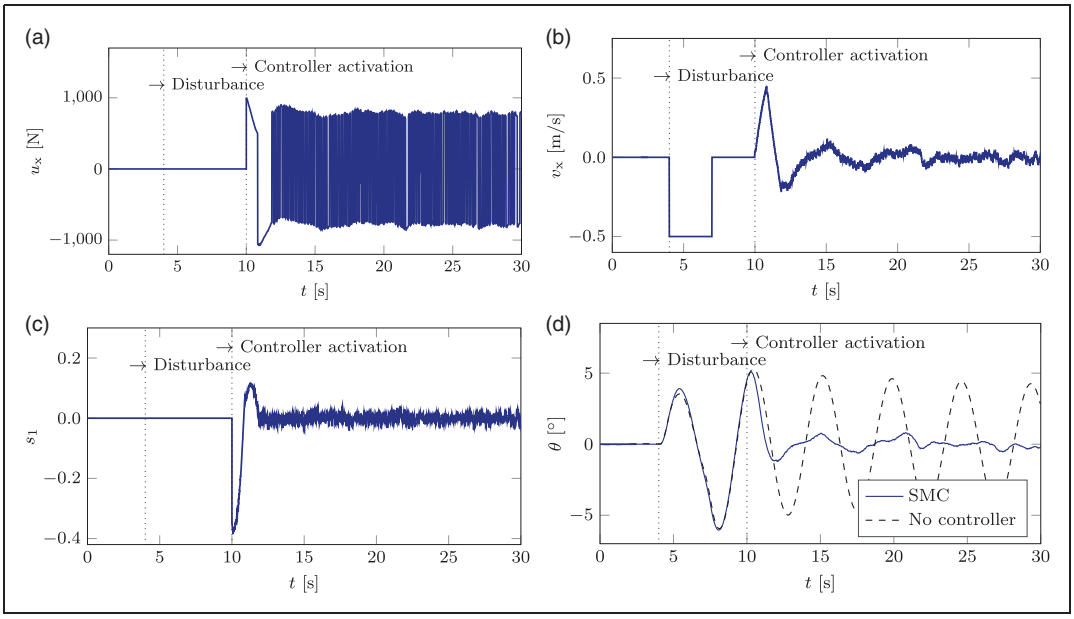

Figure 2. Stabilization of the swing angle using a discontinuous control law and $\delta_{1,2} = 2$. (a) Chattering in the control action, (b) Velocity assigned to the trolley, (c) Related switching variable and (d) Related swing angle.

performance for experiment #1 is notwithstanding portrayed together with all other experiments further on in the text.

As observed in Figure 2, even considering that the masses are exactly known, the adoption of a discontinuous term in the control law leads to the undesirable chattering phenomenon, that actually should be avoided in mechanical systems. Since the ideal relay cannot be obtained in practice, the stabilization of the swing angle is compromised. As a matter of fact, due to the persistent excitation, as shown in Figures 2(a) and 2(b), the container never comes to rest (see Figures 2(c) and 2(d)). The response related to the absence of a control action is also presented in Figure 2(d), as a reference to the efficacy of the controller.

Now, the adoption of a boundary layer is assessed. Hence, experiments $\#3_a$ to $\#6_e$ are related to the conventional but smooth sliding mode controller, that is, $\varphi_{1,2} = 0$, as before, but the boundary layer parameters are either $\phi_{1,2} = 1$ or $\phi_{1,2} = 5$. The subscripts $a, \ldots, e$ stand for the sets $\{M, m\}$ of considered values for both trolley and container masses, respectively, $\#\mathcal{E}_a = \{270, 12.9\}$ kg, $\#\mathcal{E}_b = \{270, 3.9\}$ kg, $\#\mathcal{E}_c = \{270, 21.9\}$ kg, $\#\mathcal{E}_d = \{170, 12.9\}$ kg, and $\#\mathcal{E}_e = \{370, 12.9\}$ kg, for $\mathcal{E} = 3, \ldots, 6$. The other control parameters are retained.

In respect of the intelligent sliding mode controller, the robustness against parameter variations is also investigated. First, in experiments $\#7_a$ to $\#10_e$, the adaptation rate is kept constant, $\varphi_{1,2} = 50$, and the masses are varied as before, following the same subscript scheme. The influence of $\phi_{1,2}$ and $\delta_{1,2}$ is also assessed in this set of experiments (see Table 1).

Concerning the fuzzy inference system, triangular (in the middle) and trapezoidal (at the edges) membership functions are adopted, with the central values defined as $C_i = \{-\phi_i/4, -\phi_i/20, -\phi_i/40, 0, \phi_i/40, \phi_i/20, \phi_i/4\}$. It is also important to emphasize, that in every trial the vectors of adjustable parameters are initialized with zero values, $\hat{\boldsymbol{D}}_i = \mathbf{0}$, and updated at each time step according to the adaptation law, equation (10).

In experiments #11 to #15, different values for the adaptation rate are tested: $\varphi_{1,2} = 0$ (conventional SMC), $\varphi_{1,2} = 25$, $\varphi_{1,2} = 50$, $\varphi_{1,2} = 75$, and $\varphi_{1,2} = 100$. The values of M, m, $\phi_{1,2}$ and $\delta_{1,2}$ are retained as constants in these last trials.

Since the results obtained in experiments $\#5_a$ (SMC) and $\#9_a$ (ISMC) are representative for all trials from #3 to #15, they and are shown in Figure 3.

The improved performance of the intelligent approach can be easily ascertained in Figure 3. Due to the ability of the ISMC to quickly recognize and compensate for unmodeled dynamics (friction or damping forces, for example), the proposed scheme can react in a much faster and proper way to the initial disturbance (see Figure 3(a)), which leads to a rapid reduction in the swing angle as well (see Figure 3(b)).

Indeed, the enhanced performance of the proposed ISMC over the conventional SMC holds for all experiments. This assertion can be easily confirmed in Figure 4, where the total control action $\int |v_x| \mathrm{d}t$ is plotted against the sum of absolute values of the swing angle over a fixed time interval, $\int |\theta| \mathrm{d}t$. As observed in Figure 4, the results obtained with the ISMC and the SMC are clustered in two different

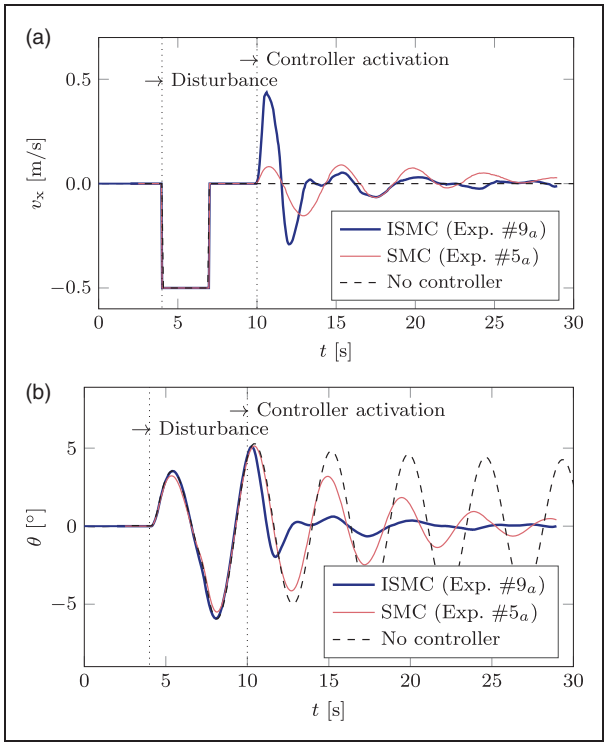

Figure 3. Comparison of the results obtained with both conventional and intelligent schemes. (a) Velocity assigned to the trolley and (b) Related swing angle.

groups, which in fact demonstrate the robustness to parametric variations of both schemes. However, while the total control action over the time related to the intelligent and the conventional approaches are comparable, the sum of the resulting swing angle obtained with the SMC is in general three times greater. Actually, the proposed intelligent controller shows an improved performance, even when compared with the discontinuous SMC (experiments #1 and #2), that is, swinging is damped out faster with comparable control effort. As mentioned before, besides the pernicious chattering phenomenon, the stabilization of the swing angle is also slightly compromised with the discontinuous control law, since the ideal relay cannot be obtained in practice. It should be emphasized that the enhanced performance of the ISMC is due to the adopted adaptive fuzzy compensation scheme, that recognizes the unmodeled dynamic effects and compensates for them.

It should be also noted that all control parameters have a physical interpretation, which in fact is a very important feature during the tuning phase. For example, η defines the convergence time to the sliding surface, λ is related to the actuator's bandwidth, φ determines how fast the fuzzy compensator will recognize the uncertainties, and ϕ is related to the trade-off between chattering and residual tracking error. This specific knowledge cannot be underestimated and,

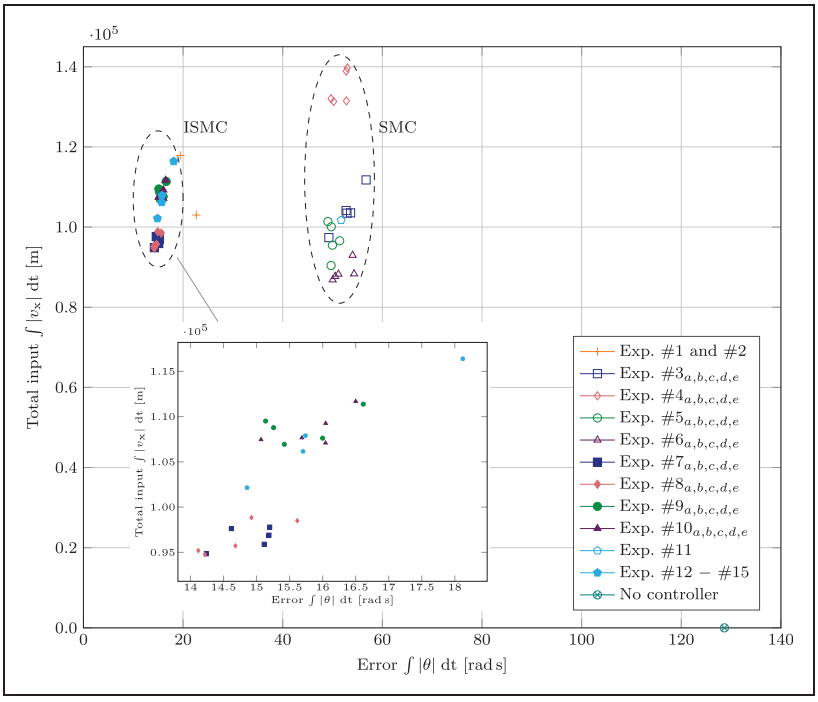

Figure 4. Comparison of the control performance for all stabilization experiments.

in fact, plays a key role in the choice of parameters, as well as in the uniformity of the resulting controller.

4.2. Trajectory tracking

In order to evaluate the tracking performance, the flatness-based model inversion solution presented in Fliess et al. (1995) is used to obtain the desired states, $\boldsymbol{q}^d$, related to the reference trajectory $\boldsymbol{p}$. Therefore,

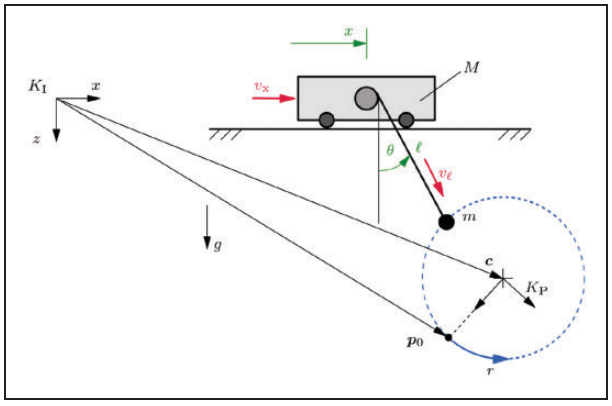

Figure 5. Coordinate systems and parameters for a circular path.

a circular path is defined in the inertial frame K_I by its initial $\boldsymbol{p}_0$ and center $\boldsymbol{c}$ points, as shown in Figure 5.

Thus, the desired trajectory is described through a parametric equation

$$\boldsymbol{p}(r) = \boldsymbol{c} + \rho \boldsymbol{S}_{IP} \begin{bmatrix} \cos(r\rho) \\ \sin(r\rho) \\ 0 \end{bmatrix}$$

where $r \in [0, r_f]$ is the adopted parameter, $\rho = ||\boldsymbol{p}_0 - \boldsymbol{c}||_2$ is the radius of the circular path, and $\boldsymbol{S}_{IP}$ is the rotation matrix from the rotating reference frame K_P to K_I.

Finally, a timing law is still required to define the trajectory. For the evaluation of the flat solution, the timing law must not only be four times continuously differentiable with respect to time but also has to ensure the required boundary conditions (Blajer and Kołodziejczyk, 2004)

$$r(t) = [126\left(\frac{t}{t_f}\right)^5 - 420\left(\frac{t}{t_f}\right)^6 + 540\left(\frac{t}{t_f}\right)^7 + - 315\left(\frac{t}{t_f}\right)^8 + 70\left(\frac{t}{t_f}\right)^9]r_f$$

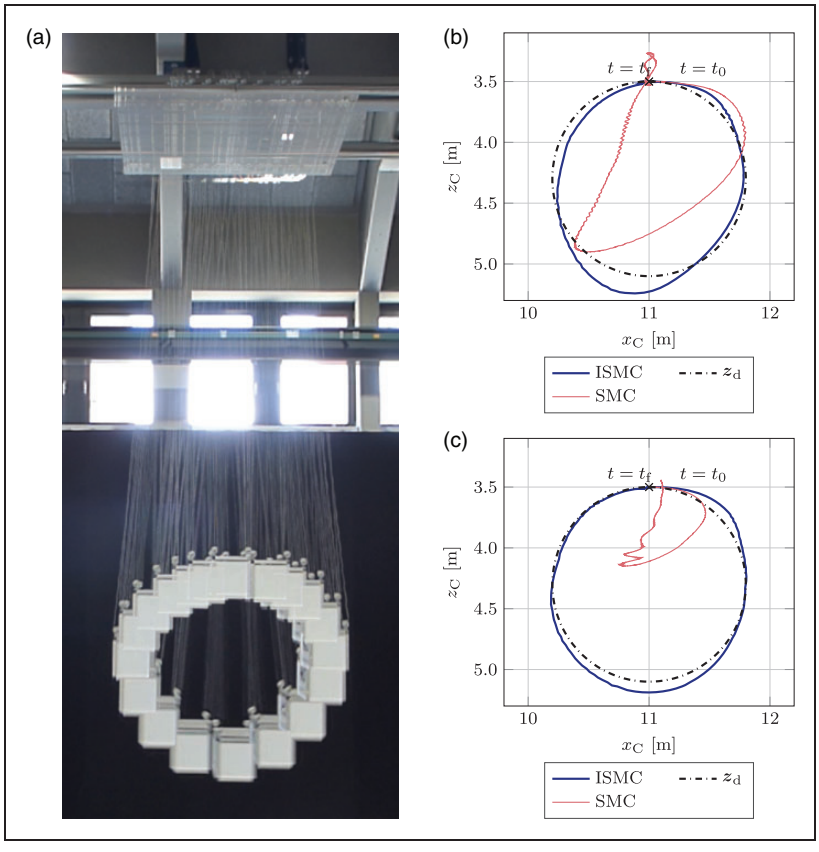

Figure 6. Tracking of a circle path. (a) Tracking with the intelligent sliding mode controller, (b) With $\phi_{1,2} = 1$ and $\delta_{1,2} = 2$ and (c) With $\phi_{1,2} = 5$ and $\delta_{1,2} = 1$.

where t_f is the time required to complete the trajectory.

First, a full circular path is chosen as desired trajectory for the container, with $r_f = 2\pi\rho$, $\boldsymbol{p}_0 = [11\ 0\ 3.5]^\top$ m, $\boldsymbol{c} = [11\ 0\ 4.3]^\top$ m, and $t_f = 15$ seconds. The other control parameters are defined according to the previous experiments: either $\#4_a$ or $\#5_a$, for the SMC, and either $\#8_a$ or $\#9_a$, for the ISMC. Figures 6 and 7 show the obtained results.

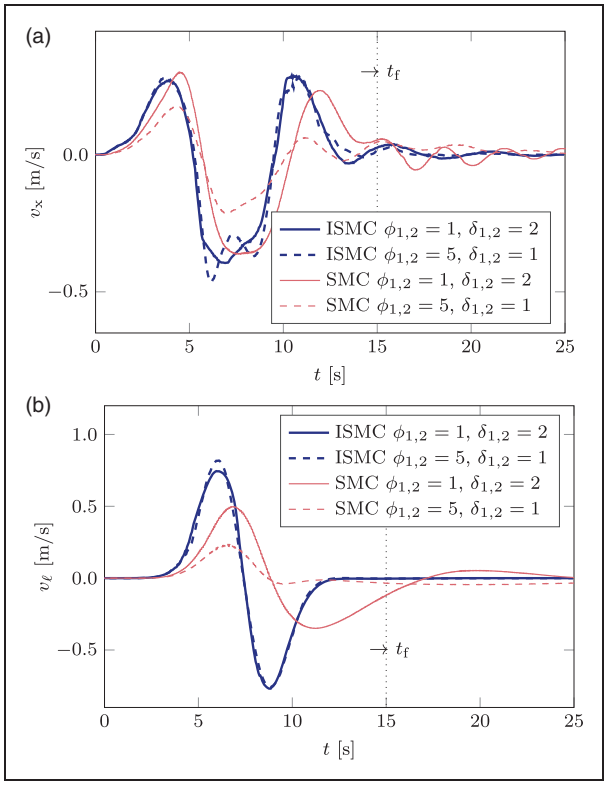

Figure 7. Control actions for the tracking of a circle path. (a) Control actions for the trolley and (b) Control actions for the cables.

By comparing the results obtained with the intelligent (ISMC) and conventional (SMC) controllers, as shown in Figures 6(b) and 6(c), the superior performance of the proposed scheme can be clearly observed. While the SMC is not able to track the prescribed trajectory, it can be seen that with both sets of parameters, the intelligent sliding mode controller could perform the task with a small associated error. The overlaid video frames presented in Figure 6(a) endorse the efficacy of the ISMC too.

It is also worth noting that the intelligent approach is less affected by variations of the chosen parameters, which as a matter of fact makes the proposed controller easier to calibrate and more robust. With respect to the ISMC, as observed in Figures 6(b) and 6(c), the trajectory tracking is visually similar for both sets of parameters adopted, which is obviously not the case with the SMC. Likewise, only the control actions related to the ISMC (see Figure 7) are not significantly changed as the control parameters are varied.

Lastly, a semicircle trajectory is also evaluated as desired trajectory, in order to illustrate that, when combined with an appropriate obstacle avoidance algorithm, the proposed intelligent controller can be safely used in automated cargo handling operations. In this case, the following parameters are taken into account for the semicircle trajectory: $r_f = \pi\rho$, $\boldsymbol{p}_0 = [9.65\ 0\ 4.5]^\top$ m, $\boldsymbol{c} = [10.6\ 0\ 4.5]^\top$ m, and $t_f = 9$ seconds. The obtained results are presented in Figures 8 and 9.

Considering a box with its centroid described by $\boldsymbol{c}$ (see Figure 8(a)), the ISMC is then employed to ensure that the container detours around the obstacle. Since the conventional sliding mode controller did not present satisfactory results for the tracking of the full

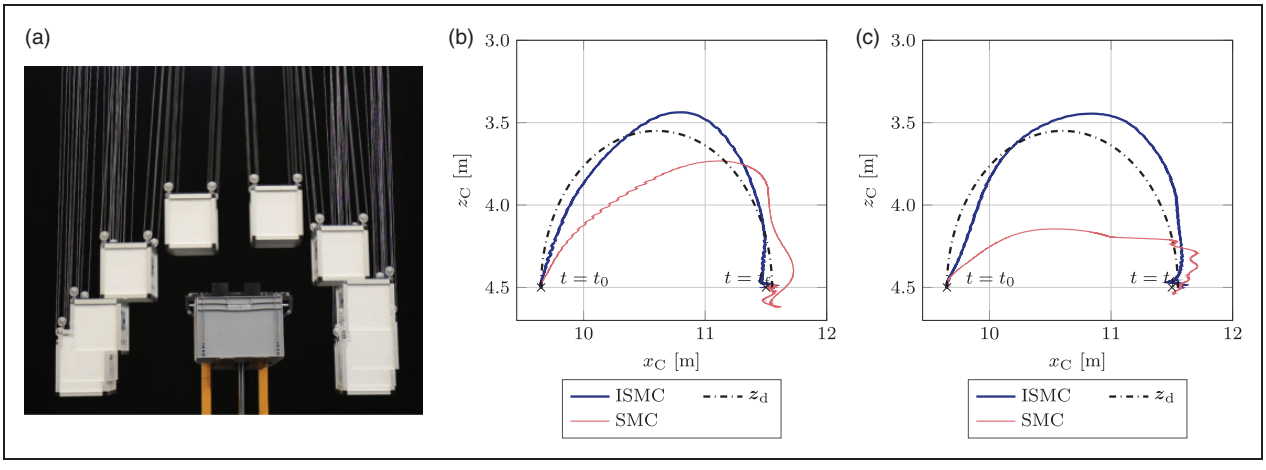

Figure 8. Tracking of a semicircle around an obstacle. (a) Tracking with the intelligent sliding mode controller, (b) With $\phi_{1,2} = 1$ and $\delta_{1,2} = 2$ and (c) With $\phi_{1,2} = 5$ and $\delta_{1,2} = 1$.

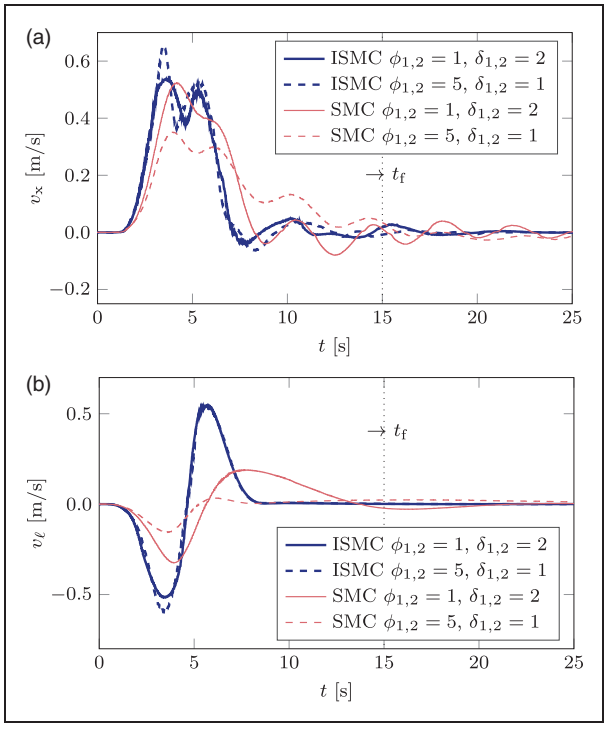

Figure 9. Control actions for the tracking of a semicircle around an obstacle. (a) Control actions for the trolley and (b) Control actions for the cables.

circle, for safety reasons, the box is omitted when the SMC was used.

Through the comparative analyses shown in Figures 8 and 9, the improved performance of the proposed intelligent sliding mode controller over the conventional counterpart can be once again confirmed. The tracking error is slightly larger than with the full circular path, since in this case the trajectory is more aggressive. The obtained results ratify the robustness of the proposed compensation scheme against modeling inaccuracies and suggest that a proper association with visual servoing (Asl et al., 2014; Al-Kaff et al., 2018) may also allow the incorporation of an obstacle avoidance feature.

5. Concluding remarks

The present paper addresses the control of multiple-input–multiple-output underactuated mechanical systems subject to modeling imprecisions and external disturbances. By combining the sliding mode technique with an adaptive fuzzy compensation scheme, a new intelligent sliding mode controller is proposed. The adoption of the switching variable instead of all state variables reduces the number of fuzzy rules and simplifies the controller design process. The convergence properties of the proposed control law are analytically proven using Lyapunov stability theory and Barbalat's lemma. In order to illustrate the feasibility of the intelligent controller, and to evaluate its efficacy, the proposed scheme is applied to an experimental container crane. The obtained results confirm the stronger improved performance of this approach for both stabilization and tracking problems. Also, the experiments show that the intelligent sliding mode controller can successfully deal with underactuated systems, even when a high level of uncertainty is involved.

Declaration of Conflicting Interests

The author(s) declared no potential conflicts of interest with respect to the research, authorship, and/or publication of this article.

Funding

The author(s) disclosed receipt of the following financial support for the research, authorship, and/or publication of this article: This work was supported by the Alexander von Humboldt Foundation (Grant Number: 3.2-BRA/1159879 STPCAPES), the Brazilian Coordination for the Improvement of Higher Education Personnel (Grant Number: BEX 8136/14-9), and the Brazilian National Council for Scientific and Technological Development (Grant Number: 308429/2017-6).

ORCID iD

Wallace M. Bessa http://orcid.org/0000-0002-0935-7730
Robert Seifried http://orcid.org/0000-0001-5795-7610

References

Al-Kaff A, Martn D, Garca F, et al. (2018) Survey of computer vision algorithms and applications for unmanned aerial vehicles. *Expert Systems with Applications* 92: 447–463.

Antsaklis PJ (2001) Intelligent control. *Wiley Encyclopedia of Electrical and Electronics Engineering*. John Wiley & Sons, Inc, 493–503.

Ashrafiuon H and Erwin RS (2008) Sliding mode control of underactuated multibody systems and its application to shape change control. *International Journal of Control* 81(12): 1849–1858.

Asl HJ, Oriolo G and Bolandi H (2014) Output feedback image-based visual servoing control of an underactuated unmanned aerial vehicle. *Proceedings of the Institution of Mechanical Engineers, Part I: Journal of Systems and Control Engineering* 228(7): 435–448.

Azimi MM and Koofigar HR (2015) Adaptive fuzzy backstepping controller design for uncertain underactuated robotic systems. *Nonlinear Dynamics* 79(2): 1457–1468.

Bencsik L, Kovács LL and Zelei A (2017) Stabilization of internal dynamics of underactuated systems by periodic servo-constraints. *International Journal of Structural Stability and Dynamics* 17(5): 1740004. DOI:10.1142/S0219455417400041.

Bessa WM (2009) Some remarks on the boundedness and convergence properties of smooth sliding mode controllers. *International Journal of Automation and Computing* 6(2): 154–158.

Bessa WM and Barrêto RSS (2010) Adaptive fuzzy sliding mode control of uncertain nonlinear systems. *Revista Controle & Automação* 21(2): 117–126.

Bessa WM, De Paula AS and Savi MA (2012) Sliding mode control with adaptive fuzzy dead-zone compensation for uncertain chaotic systems. *Nonlinear Dynamics* 70(3): 1989–2001.

Bessa WM, De Paula AS and Savi MA (2013) Adaptive fuzzy sliding mode control of smart structures. *The European Physical Journal – Special Topics* 222(7): 1541–1551.

Bessa WM, De Paula AS and Savi MA (2014) Adaptive fuzzy sliding mode control of a chaotic pendulum with noisy signals. *Zeitschrift für Angewandte Mathematik und Mechanik* 94(3): 256–263.

Bessa WM, Dutra MS and Kreuzer E (2008) Depth control of remotely operated underwater vehicles using an adaptive fuzzy sliding mode controller. *Robotics and Autonomous Systems* 56(8): 670–677.

Bessa WM, Dutra MS and Kreuzer E (2010) An adaptive fuzzy sliding mode controller for remotely operated underwater vehicles. *Robotics and Autonomous Systems* 58(1): 16–26.

Bessa WM, Kreuzer E, Krumm L, et al. (2015) Adaptive fuzzy sliding mode controller and observer for a dive cell. *Proceedings in Applied Mathematics and Mechanics* 15(1): 263–264.

Blajer W and Kołodziejczyk K (2004) A geometric approach to solving problems of control constraints: Theory and a DAE framework. *Multibody System Dynamics* 11(4): 343–364.

Blajer W and Kołodziejczyk K (2007) Control of underactuated mechanical systems with servo-constraints. *Nonlinear Dynamics* 50(4): 781–791.

Bloch A, Chang DE, Leonard N, et al. (2001) Controlled Lagrangians and the stabilization of mechanical systems II: Potential shaping. *IEEE Transactions on Automatic Control* 46(10): 1556–1571.

Bloch AM, Leonard N and Marsden J (2000) Controlled Lagrangians and the stabilization of mechanical systems I: The first matching theorem. *IEEE Transactions on Automatic Control* 45(12): 2253–2270.

Chen YF and Huang AC (2012) Controller design for a class of underactuated mechanical systems. *IET Control Theory & Applications* 6(1): 103–110.

Farrell JA and Polycarpou MM (2006) *Adaptive Approximation Based Control: Unifying Neural, Fuzzy and Traditional Adaptive Approximation Approaches*. Hoboken, NJ: John Wiley & Sons, Inc.

Fliess M, Lévine J, Martin P, et al. (1995) Flatness and defect of non-linear systems: Introductory theory and examples. *International Journal of Control* 61(6): 1327–1361.

Gómez-Estern F and der Schaft AV (2004) Physical damping in IDA-PBC controlled underactuated mechanical systems. *European Journal of Control* 10(5): 451–468.

Guo ZQ, Xu JX and Lee TH (2014) Design and implementation of a new sliding mode controller on an underactuated wheeled inverted pendulum. *Journal of the Franklin Institute* 351(4): 2261–2282.

Hou M, Duan G and Guo M (2010) New versions of Barbalat's lemma with applications. *Journal of Control Theory and Applications* 8(4): 545–547.

Hwang CL, Chiang CC and Yeh YW (2014) Adaptive fuzzy hierarchical sliding-mode control for the trajectory tracking of uncertain underactuated nonlinear dynamic systems. *IEEE Transactions on Fuzzy Systems* 22(2): 286–299.

Jang JSR, Sun CT and Mizutani E (1997) *Neuro Fuzzy and Soft Computing: A Computational Approach to Learning and Machine Intelligence*. Upper Saddle River, NJ: Prentice Hall.

Khalil HK (2001) *Nonlinear Systems*. 3rd edition. Upper Saddle River, NJ: Prentice Hall.

Kosko B (1994) Fuzzy systems as universal approximators. *IEEE Transactions on Computers* 43(11): 1329–1333.

Kovács LL and Bencsik L (2012) Stability case study of the ACROBOTER underactuated service robot. *Theoretical and Applied Mechanics Letters* 2(4): 043004. DOI: https://doi.org/10.1063/2.1204304.

Kreuzer E, Sri Namachchivaya N, Pick MA, et al. (2012) Reduced normal form approach to swing control of crane systems: Theory and experiments. *Cybernetics and Physics* 1(1): 42–50.

Li Z, Yang C, Su CY, et al. (2014) Adaptive fuzzy-based motion generation and control of mobile under-actuated manipulators. *Engineering Applications of Artificial Intelligence* 30: 86–95.

Liu Y and Yu H (2013) A survey of underactuated mechanical systems. *IET Control Theory & Applications* 7(7): 921–935.

Maghsoudi M, Mohamed Z, Tokhi M, et al. (2017) Control of a gantry crane using input-shaping schemes with distributed delay. *Transactions of the Institute of Measurement and Control* 39(3): 361–370.

Masoud ZN and Daqaq MF (2006) A graphical approach to input-shaping control design for container cranes with hoist. *IEEE Transactions on Control Systems Technology* 14(6): 1070–1077.

Muske KR, Ashrafiuon H, Nersesov S, et al. (2010) Optimal sliding mode cascade control for stabilization of underactuated nonlinear systems. *Journal of Dynamic Systems, Measurement, and Control* 134(2): 021020:1–11. DOI:10.1115/1.4005367.

Nakshatharan SS, Dhanalakshmi K and Ruth DJS (2015) Fuzzy based sliding surface for shape memory alloy wire actuated classical super-articulated control system. *Applied Soft Computing* 32(3): 580–589.

Nguyen KD and Dankowicz H (2015) Adaptive control of underactuated robots with unmodeled dynamics. *Robotics and Autonomous Systems* 64: 84–99.

Olfati-Saber R (2001) Nonlinear Control of Underactuated Mechanical Systems with Application to Robotics and Aerospace Vehicles. PhD Thesis, Massachusetts Institute of Technology, Cambridge, MA, USA. Available at: https://core.ac.uk/download/pdf/4395501.pdf (accessed 26 January 2019).

Ortega R, Spong M, Gómez-Estern F, et al. (2002) Stabilization of a class of underactuated mechanical

systems via interconnection and damping assignment. *IEEE Transactions on Automatic Control* 47(8): 1218–1233.

Otto S (2016) *Nonlinear Trajectory Control of a Gantry Crane*. Master's thesis, Institute of Mechanics and Ocean Engineering, Hamburg University of Technology.

Otto S and Seifried R (2018) Real-time trajectory control of an overhead crane using servo-constraints. *Multibody System Dynamics* 42(1): 1–17.

Park MS, Chwa D and Eom M (2014) Adaptive sliding-mode antisway control of uncertain overhead cranes with high-speed hoisting motion. *IEEE Transactions on Fuzzy Systems* 22(5): 1262–1271.

Park MS, Chwa D and Hong SK (2008) Antisway tracking control of overhead cranes with system uncertainty and actuator nonlinearity using an adaptive fuzzy sliding-mode control. *IEEE Transactions on Industrial Electronics* 55(11): 3972–3984.

Pervozvanski AA and Freidovich LB (1999) Robust stabilization of robotic manipulators by PID controllers. *Dynamics and Control* 9(3): 203–222.

Pucci D, Romano F and Nori F (2015) Collocated adaptive control of underactuated mechanical systems. *IEEE Transactions on Robotics* 31(6): 1527–1536.

Qian DW, Liu XJ and Yi JQ (2009) Robust sliding mode control for a class of underactuated systems with mismatched uncertainties. *Proceedings of the Institution of Mechanical Engineers, Part I: Journal of Systems and Control Engineering* 223(6): 785–795.

Reyhanoglu M, van der Schaft A, Mcclamroch NH, et al. (1999) Dynamics and control of a class of underactuated mechanical systems. *IEEE Transactions on Automatic Control* 44(9): 1663–1671.

Rudra S, Barai RK and Maitra M (2014) Nonlinear state feedback controller design for underactuated mechanical system: A modified block backstepping approach. *ISA Transactions* 53(2): 317–326.

Ryalat M and Laila DS (2016) A simplified IDA-PBC design for underactuated mechanical systems with applications. *European Journal of Control* 27: 1–16.

Sankaranarayanan V and Mahindrakar AD (2009) Control of a class of underactuated mechanical systems using sliding modes. *IEEE Transactions on Robotics* 25(2): 459–467.

Seifried R (2012a) Integrated mechanical and control design of underactuated multibody systems. *Nonlinear Dynamics* 67(2): 1539–1557.

Seifried R (2012b) Two approaches for feedforward control and optimal design of underactuated multibody systems. *Multibody System Dynamics* 27(1): 75–93.

Seifried R (2013) *Dynamics of Underactuated Multibody Systems: Modeling, Control and Optimal Design*. Cham, Switzerland: Springer.

Shtessel Y, Edwards C, Fridman L, et al. (2014) *Sliding Mode Control and Observation*. New York: Springer.

Singhose W, Seering W and Singer N (1994) Residual vibration reduction using vector diagrams to generate shaped inputs. *ASME Journal of Mechanical Design* 116(2): 654–659.

Slotine JJE and Li W (1991) *Applied Nonlinear Control*. Upper Saddle River, NJ: Prentice Hall.

Slotine JJ and Weiping L (1988) Adaptive manipulator control: A case study. *IEEE Transactions on Automatic Control* 33(11): 995–1003.

Spong MW (1994) Partial feedback linearization of underactuated mechanical systems. In: *IROS '94 – Proceedings of the IEEE/RSJ/GI International Conference on Intelligent Robots and Systems*, Munich, Germany, 12–16 September 1994. Piscataway, NJ: Institute of Electrical and Electronics Engineers, pp.314–321.

Spong MW, Hutchinson S and Vidyasagar M (2005) *Robot Modeling and Control*. John Wiley & Sons, Inc.

Utkin VI (1992) *Sliding Modes in Control and Optimization*. Berlin: Springer.

Wu TS, Karkoub M, Wang H, et al. (2017) Robust tracking control of MIMO underactuated nonlinear systems with dead-zone band and delayed uncertainty using an adaptive fuzzy control. *IEEE Transactions on Fuzzy Systems* 25(4): 905–918.

Wu TS, Karkoub M, Yu WS, et al. (2016) Anti-sway tracking control of tower cranes with delayed uncertainty using a robust adaptive fuzzy control. *Fuzzy Sets and Systems* 290: 118–137.

Xu L and Hu Q (2013) Output-feedback stabilisation control for a class of under-actuated mechanical systems. *IET Control Theory & Applications* 7(7): 985–996.

Xu R and Özgüner Ü (2008) Sliding mode control of a class of underactuated systems. *Automatica* 44(1): 233–241.

Yu X and Kaynak O (2017) Sliding mode control made smarter: A computational intelligence perspective. *IEEE Systems, Man, and Cybernetics Magazine* 3(2): 31–34.

Yue M, An C, Du Y, et al. (2016) Indirect adaptive fuzzy control for a nonholonomic/underactuated wheeled inverted pendulum vehicle based on a data-driven trajectory planner. *Fuzzy Sets and Systems* 290: 158–177.

Zadeh LA (1996) Fuzzy logic = computing with words. *IEEE Transactions on Fuzzy Systems* 4(2): 103–111.

Zadeh LA (2008) Is there a need for fuzzy logic? *Information Sciences* 178(13): 2751–2779.

Zhang HY, Wang J and Lu GD (2014) Self-organizing fuzzy optimal control for under-actuated systems. *Proceedings of the Institution of Mechanical Engineers, Part I: Journal of Systems and Control Engineering* 228(8): 578–590.